Journal of Power Sources 184 (2008) 84–89

Contents lists available at ScienceDirect

Journal of Power Sources

journal homepage: www.elsevier.com/locate/jpowsour

Development of 1 kW class solid oxide fuel cell stack using anode-supported planar cells

M. Yokoo*, Y. Tabata, Y. Yoshida, H. Orui, K. Hayashi, Y. Nozaki, K. Nozawa, H. Arai

NTT Energy and Environment Systems Laboratories, NTT Corporation, 3-1, Morinosato Wakamiya, Atsugi-shi, Kanagawa 243-0198, Japan

ARTICLE INFO

Article history:
Received 4 April 2008
Received in revised form 21 May 2008
Accepted 22 May 2008
Available online 8 June 2008

Keywords:
Solid oxide fuel cell
Cell stack
High electrical conversion efficiency
Durability

ABSTRACT

We have developed a 1 kW class solid oxide fuel cell (SOFC) stack composed of 50 anode-supported planar 120-mm-diameter SOFCs. Intermediate plates, which exhibited negligible deformation under operating conditions, were placed in the stack to cancel out the cumulative error related to the position and angle of the stack parts. The stack provided an electrical conversion efficiency of 54% (based on the lower heating value (LHV) of the methane used as a fuel) and an output of 1120 W when the fuel utilization, current density, and operating temperature were 67%, 0.28 A cm^{-2}, and 1073 K, respectively. The stack operated stably for almost 700 h.

1. Introduction

A power generation system using a solid oxide fuel cell (SOFC) is a promising next generation power source [1–3], since it provides high electrical conversion efficiency exceeding 50%. We have been developing an SOFC system for use in our communication bases, where electricity is more important than heat as an energy source. The key to establishing a highly efficient fuel cell system is the performances of fuel cells and cell stack that uses them. Therefore, we have been focusing on their development.

We have already developed an SOFC that provides a very high power density [4,5]. We chose an anode-supported structure because it allows the use of a thin electrolyte, which provides a low electrical resistance. A cermet consisting of nickel oxide and scandia-alumina stabilized zirconia (SASZ) is used for the anode, which has a double-layer structure [5]. For the electrolyte, we use SASZ because of its high ionic conductivity. Furthermore, lanthanum nickel ferrite (LNF), which has a high electrical conductivity and is resistant to chromium poisoning, is used as the cathode material [6–9].

We have also developed a highly efficient and durable SOFC stack with an internal manifold structure by using our anode-supported cells [10,11]. The stack, which was composed of 25 anode-supported 100-mm-diameter SOFCs, provided an output of 350 W and an electrical conversion efficiency of 56% (based on the lower heating value (LHV) of methane, which was used as a fuel). The output and efficiency were maintained for over 1100 h. The efficiency and durability of the stack were acceptable. We plan to use this cell stacking technology as a basis for providing a larger output of, for example, 1 kW.

To achieve a larger stack output, it is effective to increase the number of cells in a stack. However, as the cell number increases, errors related to the position and angle of the stack parts accumulate and thus it becomes difficult to arrange the stack parts properly. In addition, it is important to enlarge the cell size for a larger stack output. We have been trying to increase the cell diameter [5].

This paper reports the development process of a 1 kW class SOFC stack, together with advanced cell stacking technology. Furthermore, it describes the characteristics of the 1 kW class stack in detail.

2. Development strategy

The basic configuration of a 1 kW class stack is the same as that of a 350 W class stack, which is composed of 25 cells (100-mm-diameter) [10,11]. The stacks are constructed by combining many power generation units, each of which is largely composed of 1 anode-supported cell and 5 metal plates as shown in Fig. 1. The stack has one fuel feed manifold, one air feed manifold, and two fuel exhaust manifolds. The gas manifolds have strong effect on the gas distribution, which affects deviation of the voltage from cell to cell [12]. The diameter of the gas manifolds has to be large enough

* Corresponding author. Tel.: +81 46 240 2572; fax: +81 46 270 2702.
E-mail address: m.yokoo@aecl.ntt.co.jp (M. Yokoo).

0378-7753/$ – see front matter © 2008 Elsevier B.V. All rights reserved.
doi:10.1016/j.jpowsour.2008.05.083

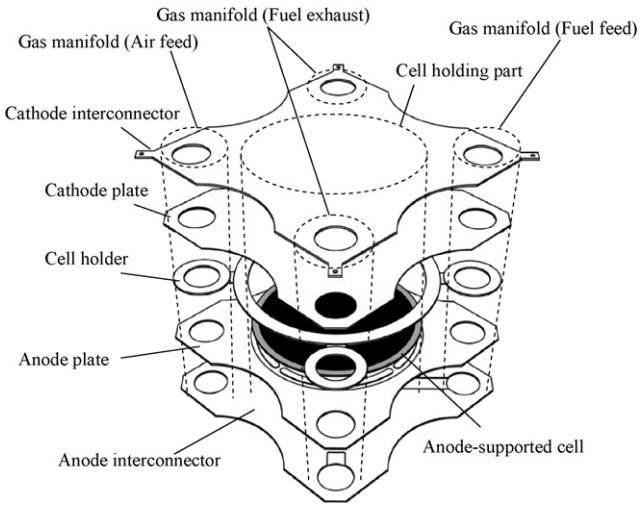

Fig. 1. Structure of power generation unit.

to achieve the uniform gas distribution [11]. The gas manifolds were designed by using the three-dimensional thermo-fluid simulator, FLUENT [13], so that the fluctuation in the flow rates of fuel and air for each cell was less than 1%. The metal plates were 1.0-mm thick. The plates were made of corrosion resistant ferritic stainless steel.

To achieve an output exceeding 1 kW, we planned to increase the number of cells in a stack from 25 to 50, and the cell diameter from 100 to 120 mm. We estimate that doubling the number of cells in a stack doubles the stack output. Furthermore, the output of each cell can be increased by about 1.5 times as a result of this increase in cell size. The detailed geometries of both cell sizes are summarized in Table 1. In this paper, we refer to cells with diameters of 100 and 120 mm as ϕ100 and ϕ120 mm cells, respectively.

We established an advanced cell stacking technology to obtain a stack with as many as 50 cells. We installed two intermediate plates, both of which were 2.5-mm thick metal plates, every 10 power generation units as shown in Fig. 2. The intermediate plates had four gas manifolds like the power generation units. In addition, the horizontal configuration of the intermediate plates was as the same as that of the power generation units. This stack is a 50-cell stack composed of the ϕ120 mm cells, which is referred to as a 1 kW class stack. The intermediate plates were installed similarly in a 50-cell stack composed of the ϕ100 mm cells. The intermediate plates exhibited negligible deformation compared with the metal plates used to construct the power generation units. The cumulative error with respect to the position and angle of the stack parts is cancelled out every 10 power generation units by the intermediate plates. By this, it is expected that all stack parts are arranged properly and thus the stacks operate well. Here, the intermediate plates were made of the same corrosion resistant ferritic stainless steel as that used for the metal plates in the power generation units.

We increased the size of the metal plates used for the power generation unit from 140 mm × 140 mm to 168 mm × 168 mm to allow the use of ϕ120 mm cells. Here, the thickness of the plates was kept at 1.0 mm. We compared the performance of single ϕ100 and ϕ120 mm cells.

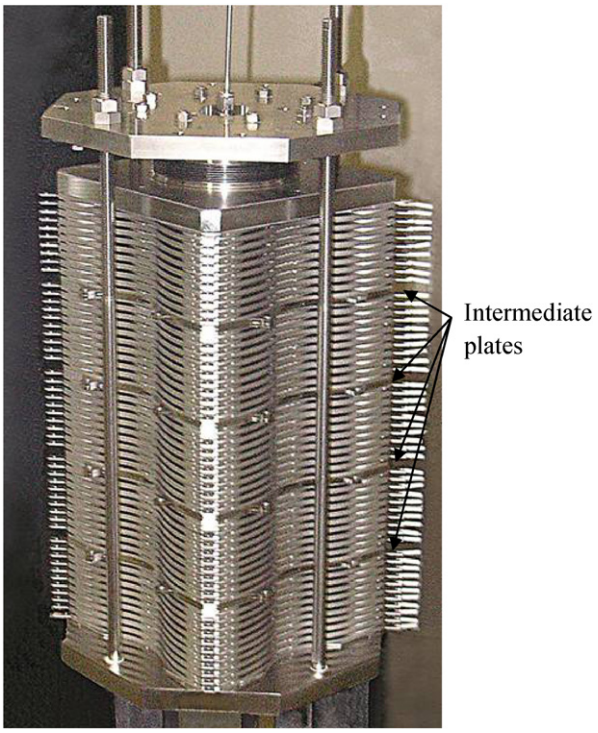

Fig. 2. 50-Cell stack with intermediate plates using ϕ120 mm cells (1 kW class stack).

We constructed 50-cell stacks with and without intermediate plates by using the ϕ100 mm cells and a 50-cell stack with intermediate plates using the ϕ120 mm cells, and we investigated their performance.

3. Experiment

The configuration of the evaluation system is shown in Fig. 3. Hydrogen and/or methane was used as fuel and dry air was used as an oxidant. When methane was used, it was reformed in a steam

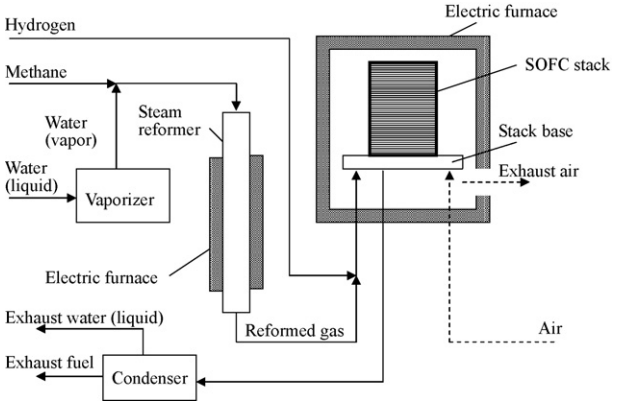

Fig. 3. Configuration of evaluation system.

Table 1
Diameter of anode, electrolyte, and cathode and active electrode area

ϕ100 mm cell				ϕ120 mm cell			
Anode	Electrolyte	Cathode	Active electrode area	Anode	Electrolyte	Cathode	Active electrode area
100 mm	100 mm	88 mm	60 cm^2	120 mm	120 mm	110 mm	95 cm^2

Table 2
Composition of reformed gas analyzed by gas chromatography (dry base)

Gas	Composition (%)
H_2	77
CO	14
CO_2	9
CH_4	–[a]

[a] Methane was below gas chromatography detection limit.

Table 3
Furnace temperatures

Electric furnace for SOFC stack			Electric furnace for steam reformer		
Top	Middle	Bottom	Inlet	Middle	Outlet
1073 K	1073 K	1073 K	923 K	1023 K	973 K

reformer and the reformed gas was fed to the stack. The steam needed for the steam reforming was generated in a vaporizer. The water flow rate was determined so that the steam to carbon ratio was 3.0. Table 2 shows the composition of the reformed gas, which we analyzed using gas chromatography (GC). Here, the water content was excluded. The methane was below the GC detection limit, which means that it was almost completely converted. The stack and steam reformer were installed in different electric furnaces both of which had three zones. Table 3 lists the temperature settings. A force was applied to the stacks by using metal bellows. Power generation tests were carried out after the anodes of the cells had been reduced by the hydrogen. The amount of current was controlled by using external electronic load equipment. Exhaust fuel from the stack was fed to a condenser to separate the water. The exhaust air from the stack was discharged into the atmosphere via a joint gap in the electric furnace.

When the cell voltage and power density were measured as a function of current density, the gas feed condition was set as shown in Table 4. When we investigated the effect of fuel utilization on stack performance, we varied the fuel flow rate while keeping the current density and air-flow rate constant.

4. Results and discussion

4.1. Establishment of advanced cell stacking technology

Fig. 4 shows the relationships between average cell voltage and current density in 50-cell stacks with and without intermediate plates. Here, ϕ100 mm cells are used in the 50-cell stacks. For comparison, the figure also shows the relationship between voltage and current density in a single ϕ100 mm cell. Hydrogen was used as the fuel for these measurements. The fuel and oxygen utilization was 60% and 15%, respectively, when the current density was 0.3 A cm^{-2}. The average cell voltages of both 50-cell stacks and the single cell voltage were almost the same at any current density, which means that the initial stack performance was acceptable for both 50-cell stacks. Temporal changes in the average cell voltage in both 50-cell stacks are shown in Fig. 5. The average cell voltage for the 50-cell stack without intermediate plates fell immediately. By contrast, the average cell voltage for the 50-cell stack with intermediate plates was maintained for the first 20 h. Furthermore, the 50-cell stack

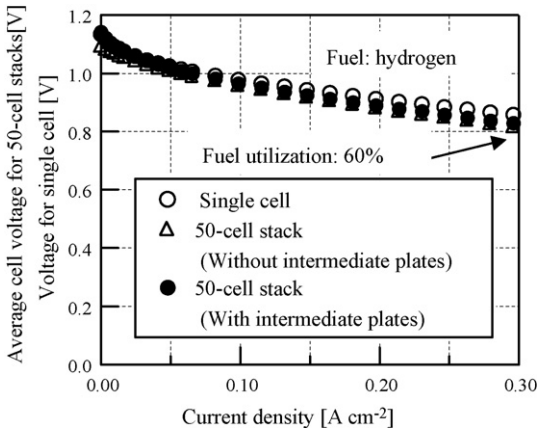

Fig. 4. Relationships between average cell voltage and current density in 50-cell stacks with and without intermediate plates and relationship between voltage and current density in single cell (cells: ϕ100 mm).

with intermediate plates operated stably for about 1200 h after this time period (not shown). These results suggest that the intermediate plates are effective as regards canceling out the cumulative error in the stack parts and arranging them properly, and thus stabilizing the stack condition and performance. This shows that successful 50-cell stacking was achieved by using the intermediate plates. Fig. 6 shows the individual cell voltages in a 50-cell stack with intermediate plates at the initial stage of the power generation test at a current density of 0.3 A cm^{-2}. The cells are numbered from the bottom. The deviation of the cell voltage δ, which was defined as follows:

$$\delta = \underset{1\le i\le 50}{\mathrm{Max}} \frac{|V_i - \bar{V}|}{\bar{V}} \times 100 \quad (1)$$

was less than 5% for the 50-cell stack. Here, V_i is the cell voltage and $\bar{V}$ is the average cell voltage.

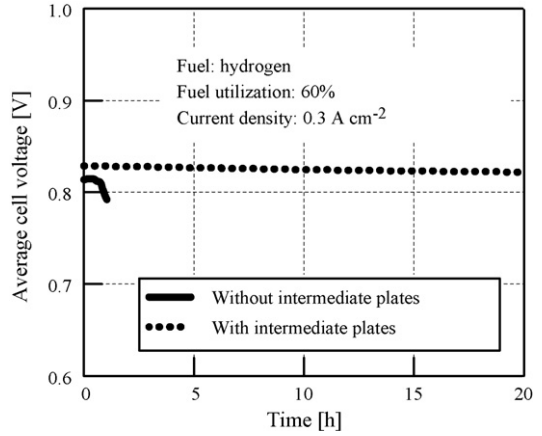

Fig. 5. Temporal changes in average cell voltage in 50-cell stacks with and without intermediate plates (cells: ϕ100 mm).

Table 4
Gas feed condition for cell voltage and power density measurement as function of current density

Hydrogen flow rate for each cell (ml min^{-1})		Methane flow rate for each cell (ml min^{-1})		Air flow rate for each cell (l min^{-1})	
Stack with ϕ100 mm cell	Stack with ϕ120 mm cell	Stack with ϕ100 mm cell	Stack with ϕ120 mm cell	Stack with ϕ100 mm cell	Stack with ϕ120 mm cell
210	315	53	79	2	3

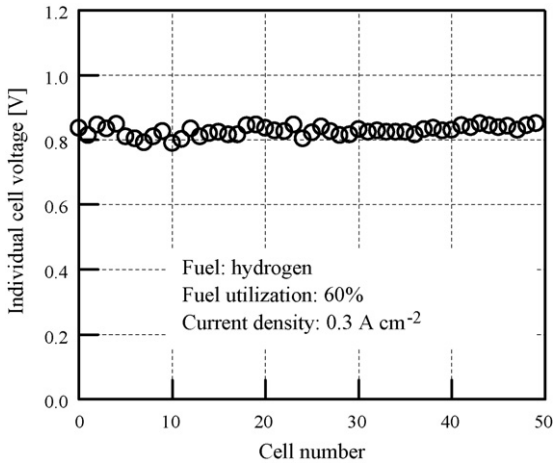

Fig. 6. Individual cell voltages in 50-cell stack with intermediate plates at initial stage of power generation test (cells: ϕ100 mm).

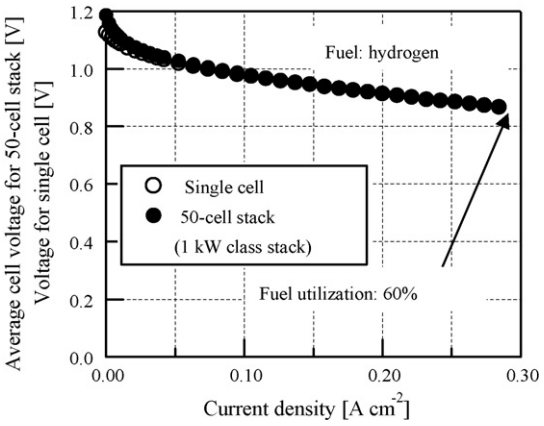

Fig. 8. Relationship between average cell voltage and current density in 50-cell stack with intermediate plates and relationship between voltage and current density in single cell (cells: ϕ120 mm, 50-cell stack using ϕ120 mm cells: 1 kW class stack).

4.2. Increased cell diameter

The relationships between voltage and current density in single ϕ100 and ϕ120 mm cells were almost the same, as shown in Fig. 7. Here, we used hydrogen as the fuel. Fuel utilization was 60% for the single ϕ100 mm cell when the current density was 0.3 A cm^{-2} and it was 60% for the single ϕ120 mm cell when the current density was 0.28 A cm^{-2}. This means the fuel utilization at the same current density was approximately the same in these two experiments. Therefore, we can conclude that both single cells provide almost the same performance.

4.3. Performance of 1 kW class SOFC stack

Fig. 8 shows the relationship between average cell voltage and current density in the 1 kW class stack, which is shown in Fig. 2. For comparison, the figure also shows the relationship between voltage and current density in a single ϕ120 mm cell. Here, the fuel was hydrogen. The fuel and oxygen utilization was 60% and 15%, respectively, when the current density was 0.28 A cm^{-2}. The performance of the single cell and 50-cell stack was almost identical. The difference between the voltage of the single cell and the average cell voltage of the 50-cell stack was 2 mV, when the current density was 0.28 A cm^{-2}. In addition, the 1 kW class stack provided a stack output of 1170 W when the current density was 0.28 A cm^{-2}. Furthermore, the average cell voltage for the 1 kW class stack was maintained for the first 90 h, as shown in Fig. 9. From these results, it can be estimated that all the stack parts in the 1 kW class stack were properly placed and functioned well. The individual cell voltages in the 1 kW class stack at the initial stage of the power generation test at a current density of 0.28 A cm^{-2} are shown in Fig. 10. There was almost no fluctuation in the cell voltages in the stack. The deviation of the cell voltage δ, which was defined by Eq. (1), was less than 1%.

The average cell voltage and power density as a function of current density in the 1 kW class stack are shown in Fig. 11. Here, methane reformed gas was fed to the stack. The fuel and oxygen utilization was 60% and 15%, respectively, when the current density was 0.28 A cm^{-2}. A stack output of 1130 W (power density: 0.24 W cm^{-2}) was achieved when the current density was 0.28 A cm^{-2}. The effect of fuel utilization was investigated in the 1 kW class stack by changing the fuel flow rate, while the current density and the oxygen utilization were kept constant. The stack output decreased with fuel utilization as shown in Fig. 12. This is because the stack voltage decreased with fuel utilization since the molar fraction of steam increased with the fuel utilization on the anode side. By contrast, the electrical efficiency at gross dc, which was calculated by using the LHV of the methane, increased with fuel utilization as shown in Fig. 12. Although the stack volt-

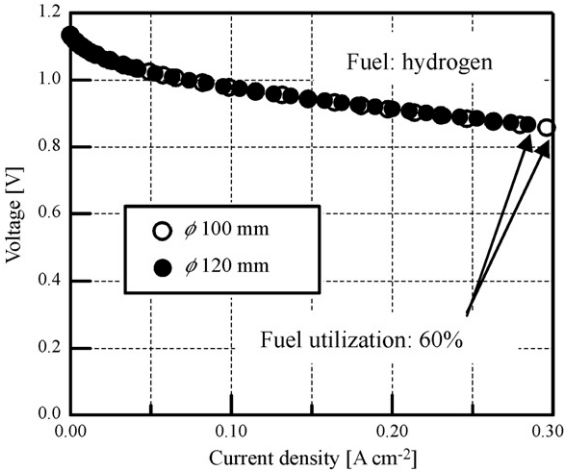

Fig. 7. Relationships between voltage and current density in single ϕ100 and ϕ120 mm cells.

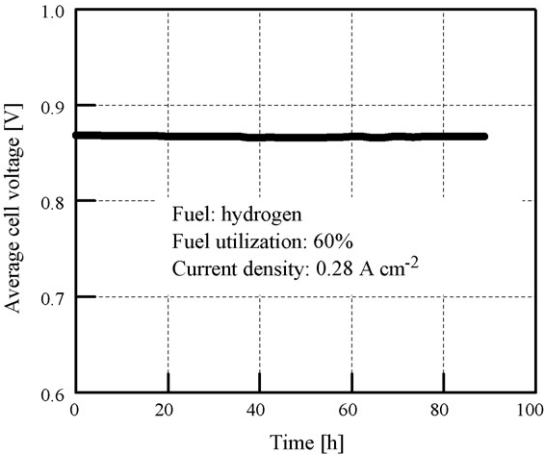

Fig. 9. Temporal change in average cell voltage in 1 kW class stack.

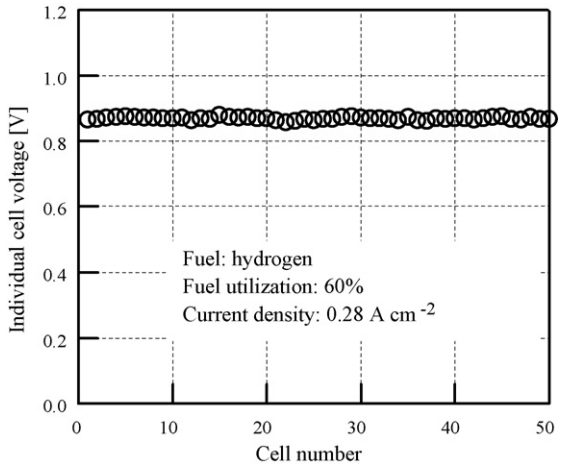

Fig. 10. Individual cell voltages in 1 kW class stack at initial stage of power generation test.

age decreased with fuel utilization, the decrement in the amount of unused fuel led to greater electrical efficiency. The stack output and electrical efficiency were 1120 W and 54%, respectively, when the fuel utilization was 67%.

The temporal change in the electrical efficiency in the 1 kW class stack is shown in Fig. 13. The current density, fuel utilization, and oxygen utilization were kept at 0.28 A cm^{-2}, 67%, and 15%, respectively. For the first 350 h, there was almost no time degradation.

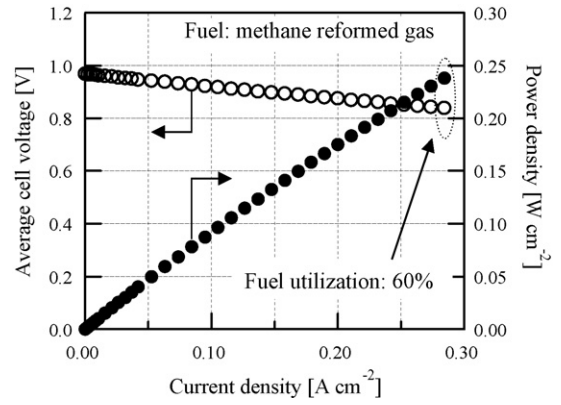

Fig. 11. Average cell voltage and power density as a function of current density in 1 kW class stack.

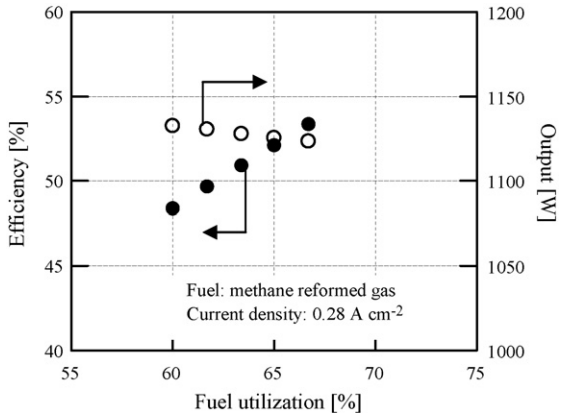

Fig. 12. Electrical efficiency at gross dc (LHV) and stack output as a function of fuel utilization in 1 kW class stack.

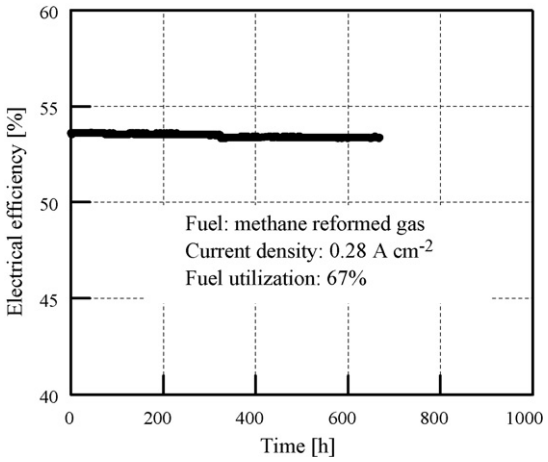

Fig. 13. Temporal change in electrical efficiency at gross dc (LHV) in 1 kW class stack.

Table 5
Summary of 1 kW class stack performance

Stack output (W)	1120
Efficiency (%)	54
Stable operating time (h)	700

However, the electrical efficiency subsequently decreased rapidly by about 0.2%. This is because the fuel (methane reformed gas) flow rate was reduced by half for about 10 min owing to mechanical trouble with the evaluation system. We consider that some cells in the stack were partially re-oxidized and their performance degraded slightly. However, stable stack operation was maintained after the trouble. As a result, the stack operated stably for about 700 h. In the 1 kW class stack, no efficiency drop of greater than 0.1% was observed except for that caused by the problem with the system. The 1 kW class stack performance is summarized in Table 5.

5. Conclusion

We developed a 1 kW class SOFC stack composed of 50 anode-supported planar 120-mm-diameter SOFCs. We used intermediate plates to establish an advanced cell stacking technology that allows us to stack 50 cells. The cumulative error with respect to the position and angle of stack parts was cancelled out by the intermediate plates. The 1 kW class stack provided an electrical conversion efficiency of 54% (based on the LHV of methane, which was used as a fuel) and an output of 1120 W when the fuel utilization, current density, and operating temperature were 67%, 0.28 A cm^{-2}, and 1073 K, respectively. The stack operated stably for almost 700 h. No efficiency reduction of greater than 0.1% was observed except for that caused by system trouble.

References

[1] T. Ujiie, ECS Transactions 7 (2007) 3–9.
[2] W.A. Surdoval, ECS Transactions 7 (2007) 11–15.
[3] B. Rietveld, ECS Transactions 7 (2007) 17–23.
[4] H. Orui, K. Watanabe, R. Chiba, M. Arakawa, Journal of Electrochemical Society 151 (2004) A1412–A1427.
[5] H. Orui, K. Nozawa, R. Chiba, T. Komatsu, K. Watanabe, S. Sugita, H. Arai, M. Arakawa, ECS Transactions 7 (2007) 225–261.
[6] R. Chiba, F. Yoshimura, Y. Sakurai, Solid State Ionics 124 (1999) 281–288.
[7] T. Komatsu, H. Arai, R. Chiba, K. Nozawa, M. Arakawa, K. Sato, Electrochemical and Solid State Letters 9 (2006) A9–A12.
[8] T. Komatsu, H. Arai, R. Chiba, K. Nozawa, M. Arakawa, K. Sato, Journal of Electrochemical Society 154 (2007) B379–B382.

[9] R. Chiba, H. Orui, T. Komatsu, Y. Tabata, K. Nozawa, H. Arai, M. Arakawa, K. Sato, ECS Transactions 7 (2007) 1191–1200.
[10] Y. Tabata, M. Yokoo, Y. Yoshida, K. Hayashi, K. Nozawa, Y. Nozaki, H. Arai, Proceedings of the 2007 Fuel Cell Seminar and Exposition, 2007, p. 222.
[11] M. Yokoo, Y. Tabata, Y. Yoshida, K. Hayashi, K. Nozawa, Y. Nozaki, H. Arai, Journal of Power Source 178 (1) (2008) 59–63.
[12] A.C. Burt, I.B. Celik, R.S. Gemmen, A.V. Sminov, Journal of Power Source 126 (1) (2004) 76–87.
[13] T.M. Prinkey, A.W. Rogers, S.R. Gemmen, American Society of Mechanical Engineering Heat Transfer Division 369 (4) (2001) 291–300.